solestial

DRD3 CERN

# Defects Induced by 1 MeV Electron and $^{60}$Co-Gamma Irradiation in Boron-Doped Silicon

**Authors:** Yana Gurimskaya[1,2]; Michael Moll[1]; Niels Sorgenfrei[1,3], Vendula Maulerova -Subert[1,4], Moritz Wiehe[1]

**Co-authors**: Alex Fedoseev[2], Stanislau Herasimenka[2], Mikhail Reginevich[2]

[1]CERN, Geneva, Switzerland
[2]Solestial, Inc., Tempe, Arizona, USA
[3]Albert Ludwigs Universität Freiburg, Freiburg, Germany
[4]Hamburg University, Hamburg, Germany

**Session Classification:** **WG3/WP3 - Extreme fluence and radiation damage characterization: WG3 scientific talks**

*CERN KT Collaboration Agreement KN5705/KT/EP/263C*

# p-type Si to extreme fluences

## WG3/WP3: Extreme fluence and radiation damage characterization

- pursue the “acceptor removal project” to understand defect kinetics mechanisms
- measure the ratio of point to cluster defects for various particle irradiations → input to NIEL studies
- compare microscopic defect formation to macroscopic effects on Si sensors and Si solar cells for space

**‘Acceptor removal’:**

- De-activation of B as a shallow dopant with irradiation, leading to the change of $N_{eff}$ determined by $V_{dep}$ on the macroscopic level
- Originated from Boron-Containing Defect (BCD) formation (*see presentations by Andrei Nitescu and Kevin Lauer*)

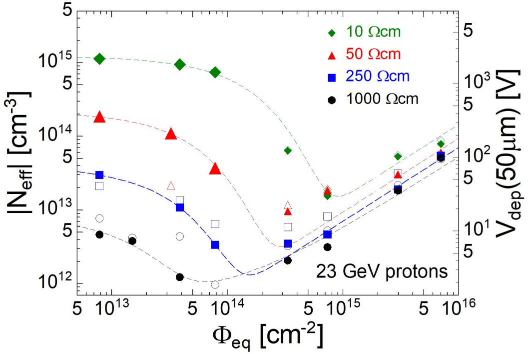


Hand-by-hand with NIEL project (*see presentation by Vendula Maulerova-Subert*)

**AIM**: Evaluation of the concept to produce a 2-parameter NIEL scaling, i.e. two ‘hardness factors’ coming up for point and cluster defect formations able to describe the macroscopic ‘NIEL violation’ observations and to develop universal TCAD defect model combining proton, neutron and electron damage

# Primary displacement damage in Si

## Damage mechanism

Non-ionising damage results from direct collisions of incident particle with atomic nuclei of the crystal lattice, creating primary defects via such mechanisms:

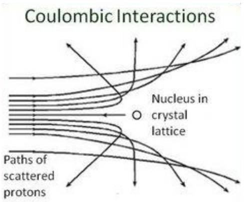


Dominates at particle energies <10 MeV, producing isolated defects

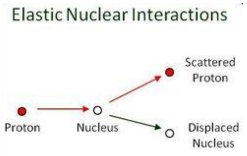


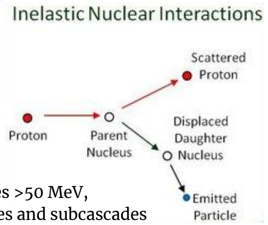


Dominant at energies >50 MeV, formation of cascades and subcascades

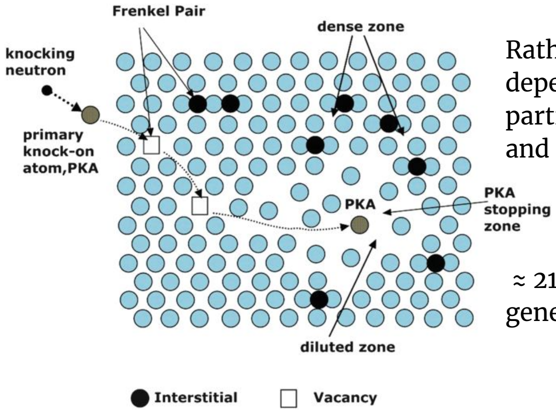


Rather complex process, depends on incident particle mass, charge and energy

≈ 21 eV needed to generate Frenkel pair

## Defect formation simulations

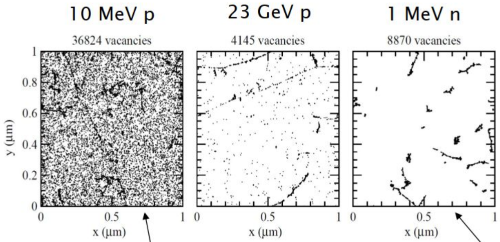


Primary defects homogeneously scattered over large volume.

Primary defects densely clustered in small volume.

Initial distribution of vacancies produced by 10 MeV protons, 23 GeV protons and 1 MeV neutrons . The plots are projected over 1 $\mu$m depth (z) and correspond to a fluence of 1E+14 particles/cm².

DOI: 10.1016/S0168-9002(02)01227-5

## Going less complex:

Damage exclusively attributed to point defects:

- $^{60}$**Co gamma** rays (Compton electron with $E_{max}$ of 1 MeV)
- 1 MeV **electrons** (space conditions)

# Microscopic damage: $N_{BiOi}/\Phi_{neq}$

*Widely used in community*

**TSC**

**I-DLTS**

*Used at CERN*

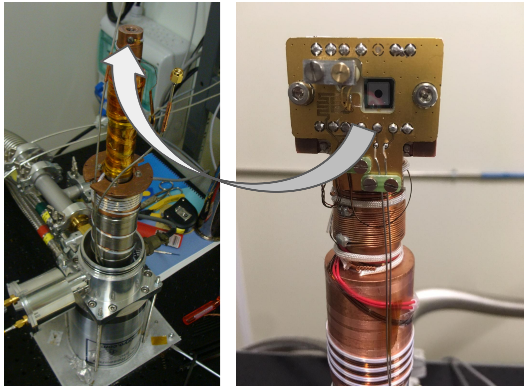

**C-DLTS**

*Widely used in community*

**TS-Cap**

*Used by Hamburg group*
*Implementing at CERN*

I-DLTS looks into the current transient by carrier emission in a time scale of milliseconds (TSC - seconds, different filling procedure). TSC and I-DLTS can be complementary to each other by means of defect identification. Both - current-based microscopic defect analysis methods.

**Defects mapping**

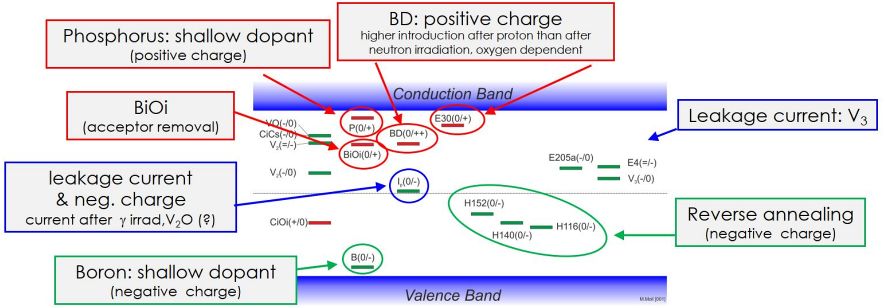


Find the microscopic origin of the macro effects of radiation damage such as $I_{leak}$, trapping and doping

Up to $V_{bias}$ 300V

**TSC**

**I-DLTS**

Max $V_{bias}$ 100V

**C-DLTS**

1 MHz AC signal
Max $V_{bias}$ 100V

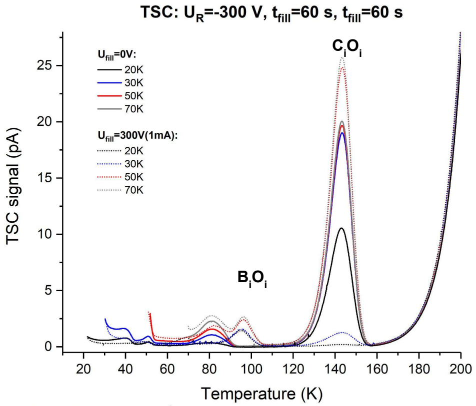


CIS16-CZ-06-150-DS-81_1E+15 e/cm²

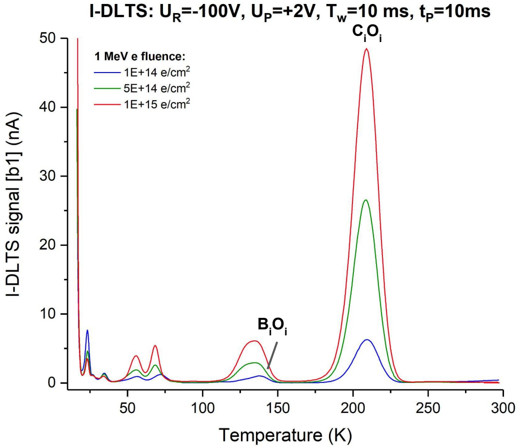


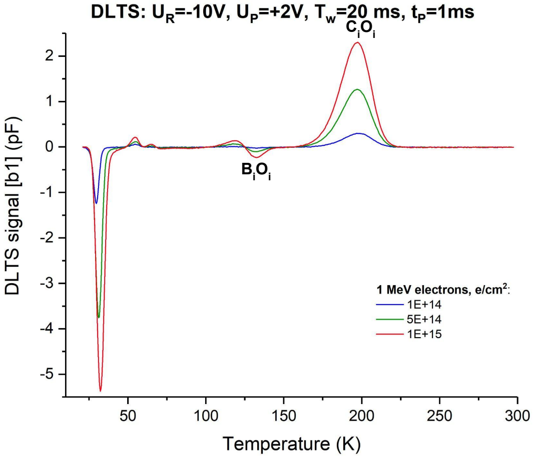


**CZ pad diodes of 120 Ω·cm irradiated with 1 MeV electrons**

⊕
- Bias voltage up to 300V;
- Appearance of defects with T-dependent $\sigma$ by $T_{fill}$ variation - multi-phonon capture process;
- 'Full' concentrations;

⊖
- Noise;
- High $I_{leak}$ from 180K.

⊕
- Can detect shallow defect levels, at least 8 in total;
- Arrhenius in one T-scan;
- Separate type of carriers;

⊖
- Amplitude of transient is T-dependent.

⊕
- Terrific sensitivity, at least 7 defect levels in total;
- No need to fully deplete device;
- Separate type of carriers;

⊖
- Limitation: $N_T \ll N_S$;
- Carrier freeze-out.

# Test structures

| Sensor name | Thickness, µm | Fluence, e/cm² | Facility |
|---|---|---|---|
| CZ-03-72 | 50 | 5E+14 | MP |
| CZ-03-71 | 50 | 1E+15 | MP |
| CZ-06-54 | 150 | 1E+14 | CEA |
| CZ-06-67 | 150 | 5E+14 | CEA |
| CZ-06-81 | 150 | 1E+15 | CEA |
| CZ-03-48 | 350 | 1E+14 | MP |
| CZ-03-51 | 350 | 5E+14 | MP |
| CZ-03-49 | 350 | 1E+15 | MP |
| CZ-03-92 | 50 | 200 kGy | RBI |
| CZ-03-93 | 50 | 1 MGy | RBI |

DRD3 solestial CERN

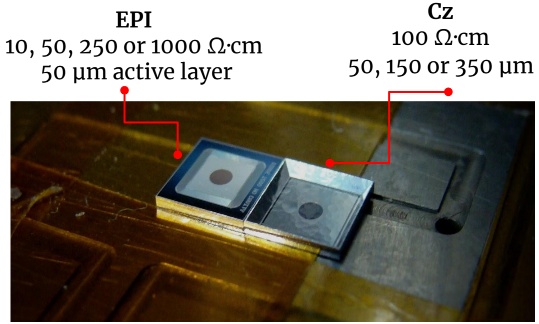


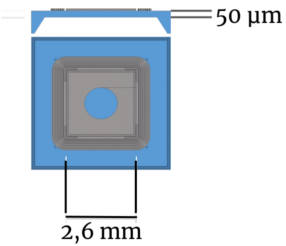


CiS Forschungsinstitut für Mikrosensorik GmbH

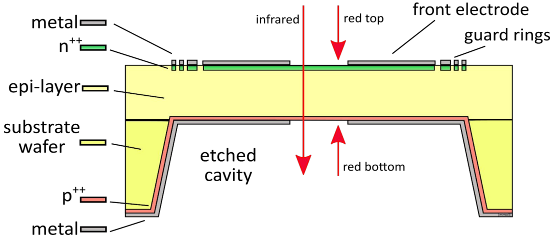


*The schematics of the cross section of Si test structure for defect spectroscopy measurements and indication of different illumination configuration. Dimensions not to scale.*

## Electron irradiation

1 MeV: 1E+14, 5E+14, 1E+15 e/cm²

MercuryPlastics

cea ines INSTITUT NATIONAL DE L'ENERGIE SOLAIRE

## $^{60}$Co γ – irradiation

200 kGy and 1 MGy

Institut Ruđer Boškovi

EURO-LABS EUROPEAN LABORATORIES FOR ACCELERATOR BASED SCIENCES

This project has received funding from the European Union's Horizon Europe Research and Innovation programme under Grant Agreement No 101057511.

# Example of C-DLTS measurements

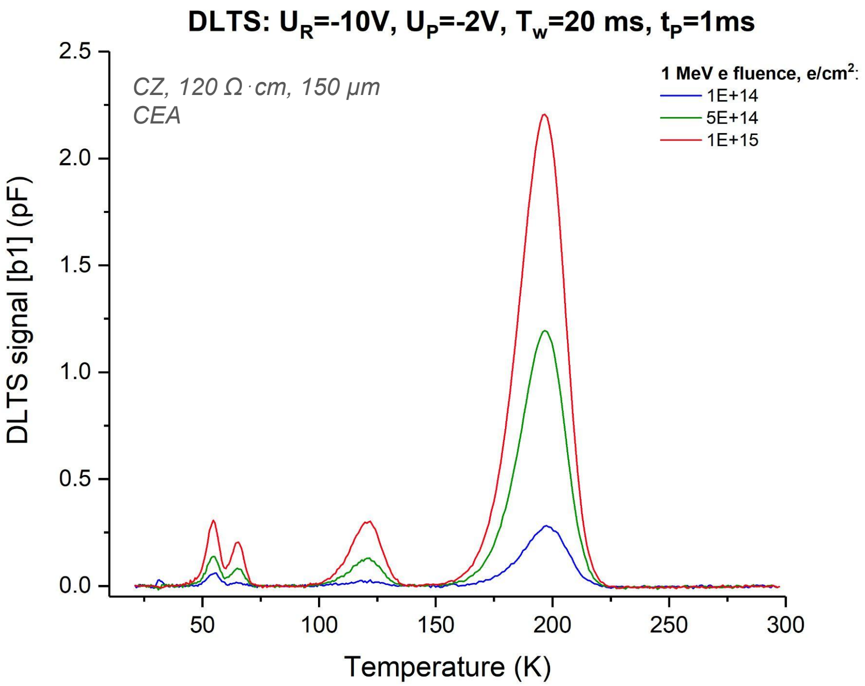


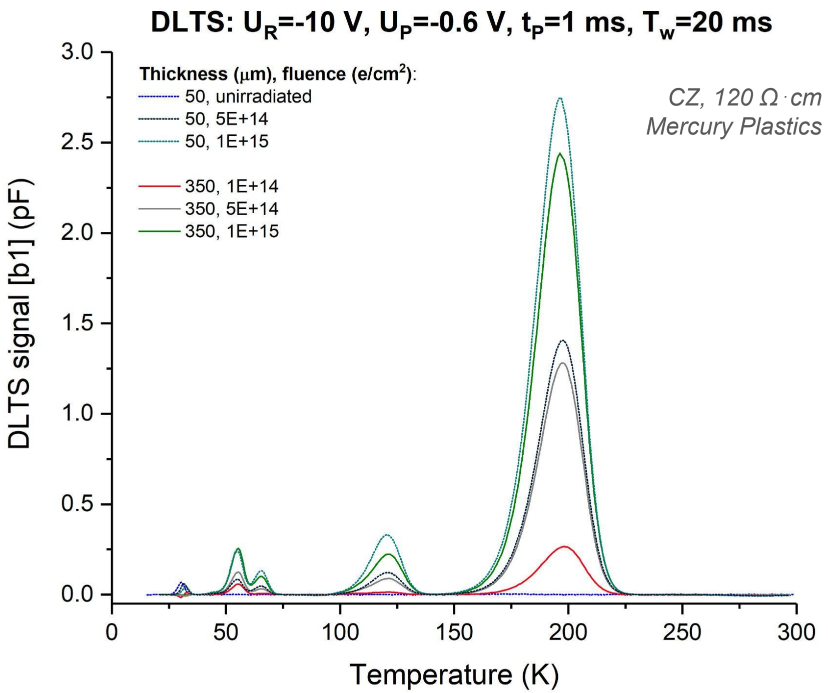


Identical defect levels are detected for all *e*-irradiated test structures from both facilities for all thicknesses, defect concentrations (~peak amplitudes) increase with fluence

# Example of DLTS analysis

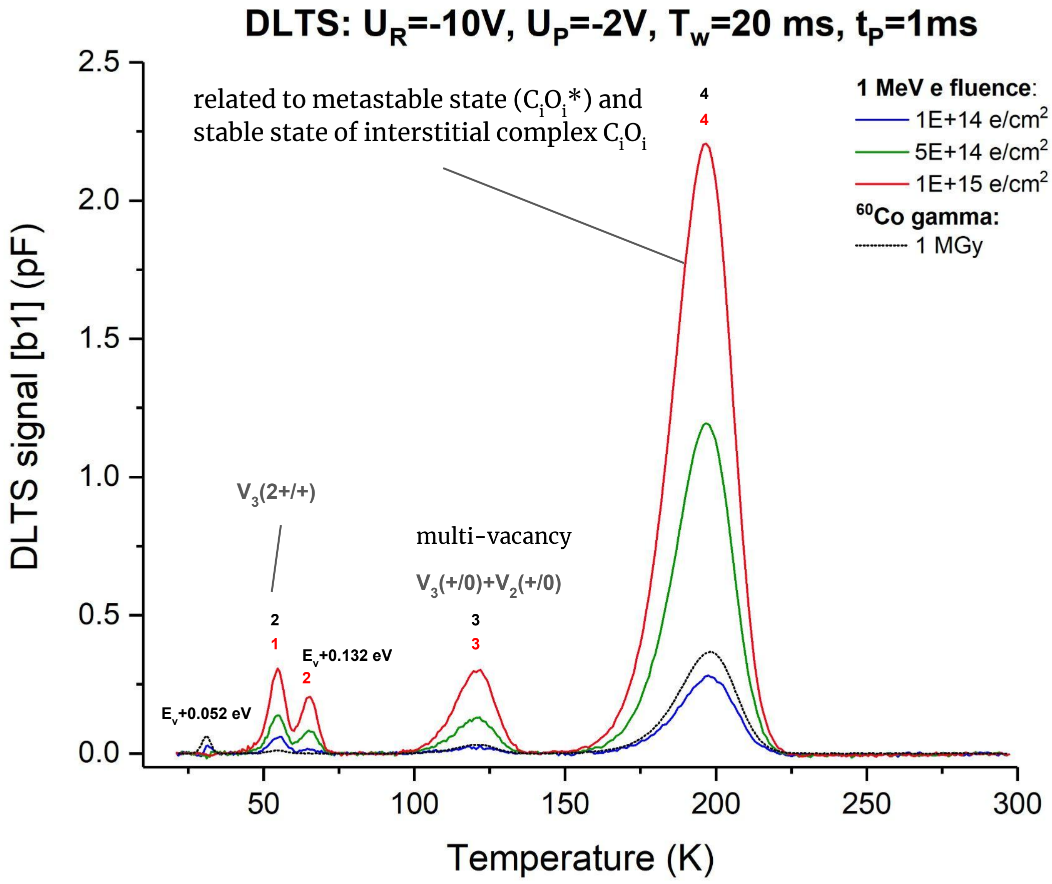


Uses 28 correlator functions to build Arrhenius

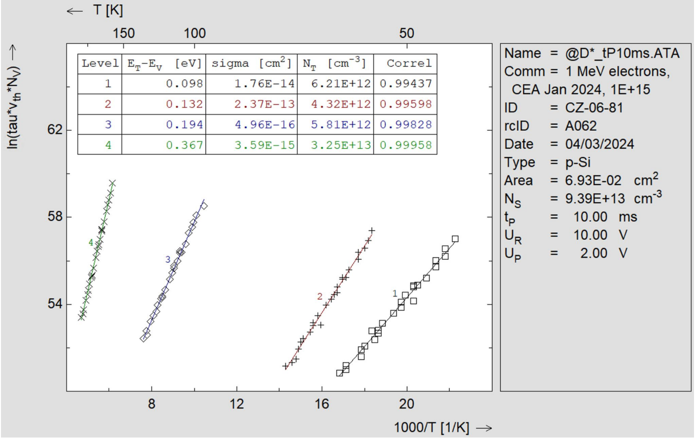


| Defect type, name | Activation energy, eV | Sigma, cm² | Concentration, cm⁻³ |
|---|---|---|---|
| H33K* | 0.052 | - | 9.4E+11 |
| H55K | 0.098 | 1.9E-14 | 3.1E+12 |
| H65K | 0.132 | 2.4E-13 | 2.9E+12 |
| H120K | - | - | - |
| | 0.194 | 4.7E-16 | 4.5E+12 |
| H196K | 0.334 | 6.6E-16 | 8.5E+12 |
| | 0.362 | 2.5E-15 | 5.1E+13 |
| E133K | 0.238 | 3.7E-15 | 2.8E+12 |

H33K* detected below carrier freeze-out
E133K ≈ $B_iO_i$

# T-dependent capture cross section and Poole-Frenkel effect

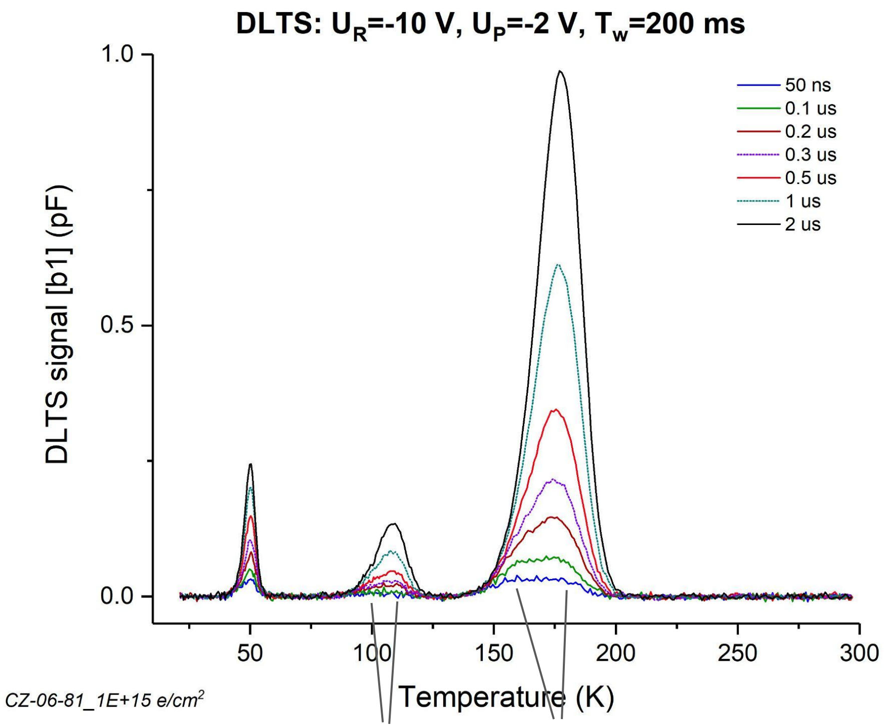


Presence of 2 peaks visible with short pulses

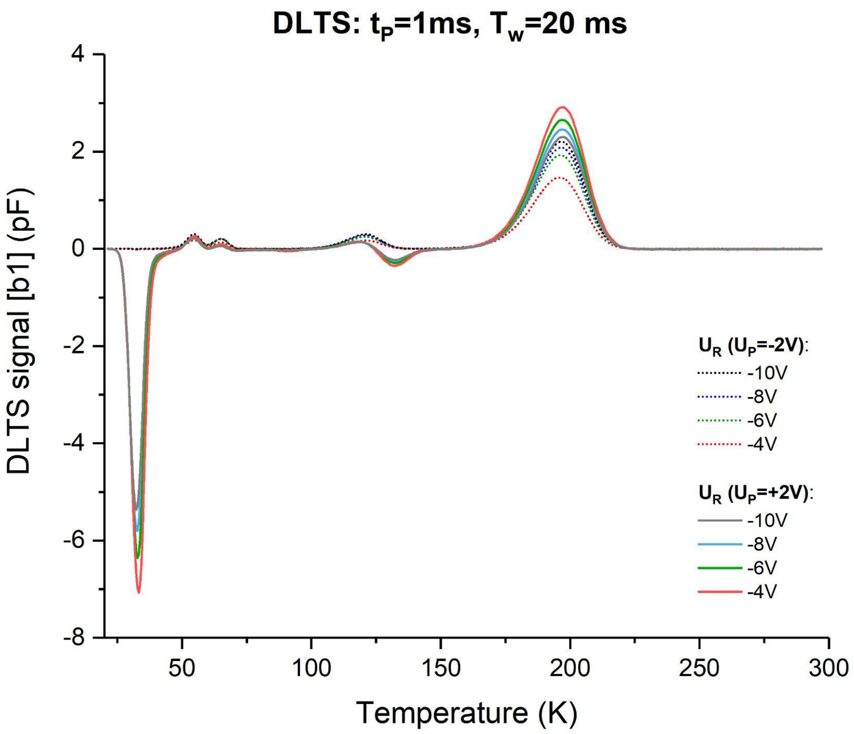


Poole-Frenkel gives a hint of charge state of the defect

# Reverse capacitance – compensation for CZ

C-V(*f*) at 150K and TS-Cap combined with TSC are planned

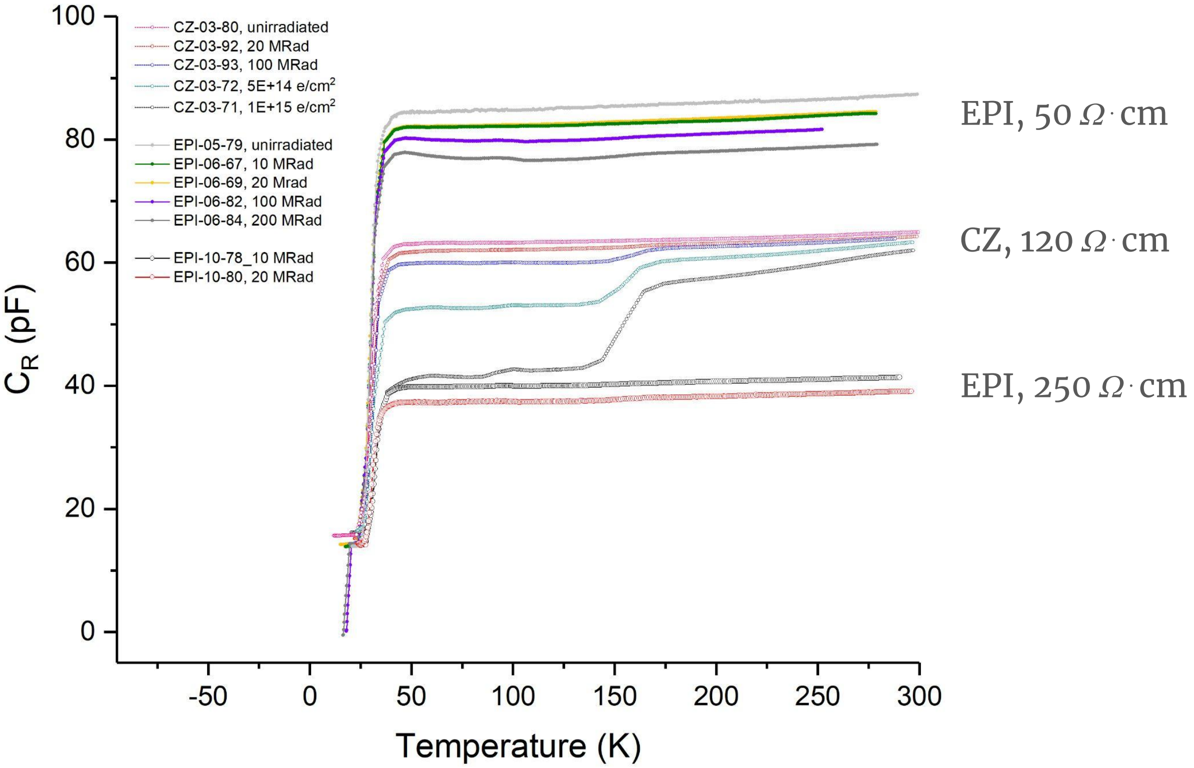


Measurements are performed at 1MHz frequency during DLTS scan - defect cannot follow and 'freeze out'

# Example of TSC measurements

Majority carrier injection → hole traps

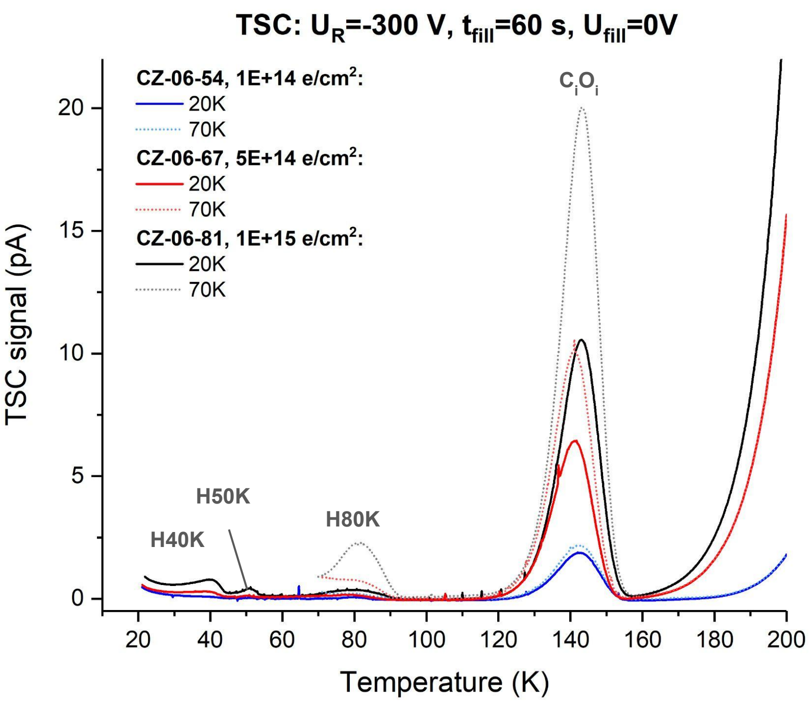


Both carrier types injection → electron and hole traps

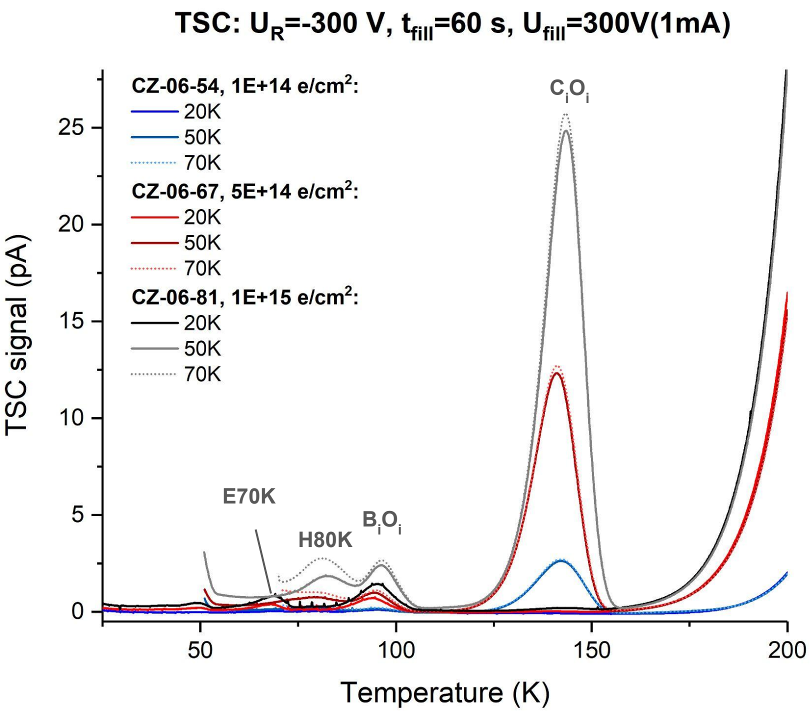


Integration over the peak gives us charge → defect concentration, see slide 13 for summary

# Example of I-DLTS measurements

Majority carrier injection → hole traps

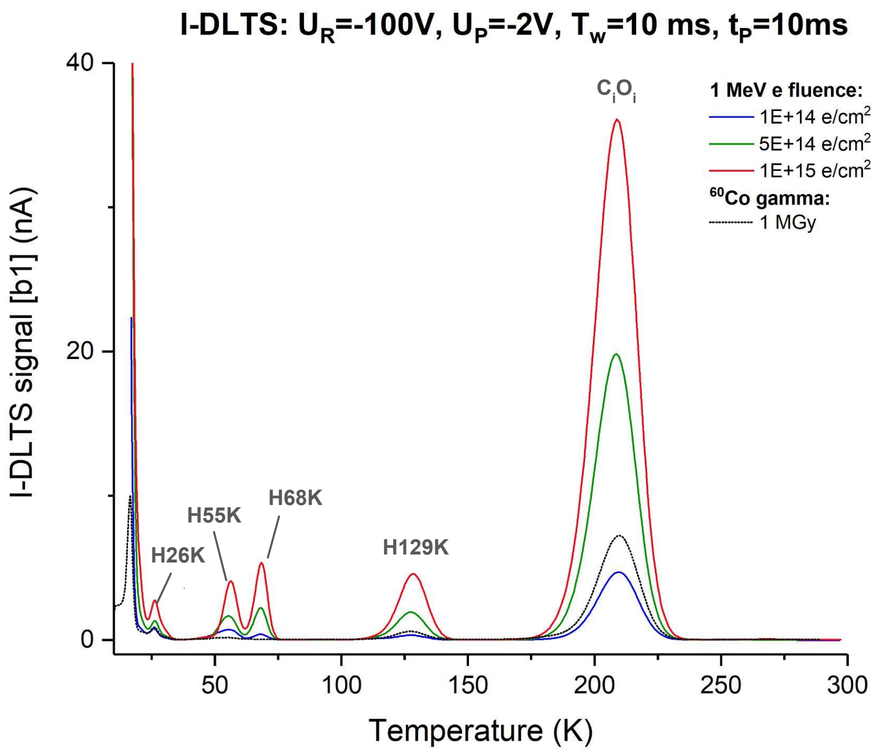


Both carrier types injection → electron and hole traps

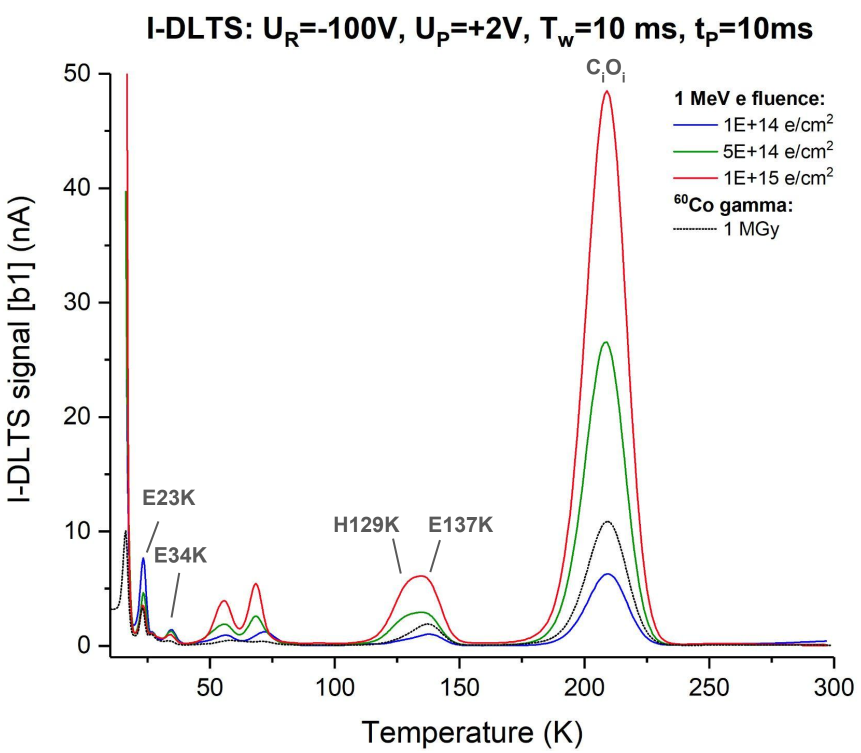


Can detect at least 8 defect levels, has power of C-DLTS but gives under-estimation in concentrations ←T-dependent I-DLTS amplitude

# Data comparison over 3 methods for 1E+15 e/cm² fluence

DRD3 solestial CERN

| $E_{a\_DLTS}$, eV | $\sigma_{\_DLTS}$, cm² | $N_{t\_DLTS}$, cm⁻³ | $E_{a\_I\text{-}DLTS}$, eV | $\sigma_{\_I\text{-}DLTS}$, cm² | $N_{t\_I\text{-}DLTS}$, cm⁻³ | $N_{t\_TSC}$, cm⁻³ | Defect | γ |
|---|---|---|---|---|---|---|---|---|
| | | | 0.031 | 3.4E-15 | 1.8E+12 | | | yes |
| 0.052 | - | 9.4E+11 | 0.048 | 2.5E-15 | 5.2E+11 | | | yes |
| 0.098 | 1.9E-14 | 3.1E+12 | 0.092 | 1.6E-14 | 1.7E+12 | 3.1E+11 | $V_3^{(2+/+)}$ | yes |
| 0.132 | 2.4E-13 | 2.9E+12 | 0.126 | 9.2E-14 | 2.5E+12 | | | no |
| 0.19 | 1E-15 | - | | | | | $V_3^{(+/0)}$ | - |
| 0.194 | 4.7E-16 | 4.5E+12 | 0.193 | 4.6E-16 | 2.7E+12 | 2.8E+12 | $V_2^{(+/0)}$ | yes |
| 0.334 | 6.6E-16 | 8.5E+12 | | | | | $C_iO_i^*$ | - |
| 0.362 | 2.5E-15 | 5.1E+13 | 0.357 | 1.8E-15 | 2.2E+13 | 2.21E+13 | $C_iO_i^{(+/0)}$ | yes |
| 0.238 | 3.7E-15 | 2.8E+12 | 0.243 | 1.57E-15 | 2.7E+12 | 1.74E+12 | $B_iO_i^{(0/-)}$ | yes |

Markevich et al, V3 and V3-O family of defects in Si (2014)
Makarenko et al, Formation of bistable I-complex in irradiated p-Si (2019)

- Good match over 3 techniques for isolated point defect levels but not for superimposed defect signals, have to be treated with care.
- Isochronal annealing (and/or forward current injection annealing) planned.
- Optical injection is in implementation.

# Ratios of introduction rates for dominant defects after 1 MeV electrons and $^{60}$Co-gammas

| Fluence[e/cm²] | $\frac{[B_iO_i^{(+/0)}]}{[C_iO_i^{(+/0)}]}$ |
|---|---|
| 1E+14 | 0.068 |
| 5E+14 | 0.0558 |
| 1E+15 | 0.0561 |
| **Dose [10⁶ Gy]** | $\frac{[B_iO_i^{(+/0)}]}{[C_iO_i^{(+/0)}]}$ |
| 0.2 | 0.211 |
| 1 | 0.159 |

PRELIMINARY

- For electron irradiation ratio $B_iO_i/C_iO_i$ is fluence independent, ~0.06.
- For γ-irradiation: dose dependence → higher dose- less $B_iO_i$ relatively to $C_iO_i$.
- For EPI (γ): 250 Ωcm - $IR_{BiOi}$ and $IR_{CiOi}$ almost equal, 50 Ωcm - $IR_{BiOi}$ is higher than $IR_{CiOi}$. [A.Himmerlich, 40th RD50 Workshop]

# Outlook

- It was shown that radiation damage is a complex process not yet fully understood;
- A combination of several experimental methods (TSC, TS-Cap, I-DLTS, C-DLTS, others) is essential to investigate microscopic defect formation for various particle irradiations especially at high fluences and for high resistivity material;
- Isochronal annealing and forward current injection studies are planned;
- Optical injection option should be implemented to overcome the drawback of uncertainties in traditional voltage pulse filling with forward bias $I_{fill}$ in both I-DLTS and TSC;
- Full hardware and software in place, problem with LED triggering to be solved.

**Thank you!**